Midkine inhibitor (iMDK) induces apoptosis of primary effusion lymphoma via G2/M cell cycle arrest

Mikinori Ueno[a,d], Ryusho Kariya[a], Sittithumcharee Gunya[a,b], Kodcharat Cheevapruk[a,b,c], Seiji Okada[a,b,*]

Division of Hematopoiesis, [a]Joint Research Center for Human Retrovirus Infection, [b]Graduate School of Medical Sciences, Kumamoto University, 2-2-1 Honjo, Chuo-ku, Kumamoto, 860-0811, Japan

[c]Department of Pharmacology, Faculty of Medicine Siriraj Hospital, Mahidol University, Bangkok 10700, Thailand

[d]Current address: Graduate School of Fisheries and Environmental Studies, Nagasaki University, 1-14 Bunkyo-machi, Nagasaki, 852-8521, Japan

*Corresponding author. Division of Hematopoiesis, Joint Research Center for Human Retrovirus Infection, Graduate School of Medical Sciences, Kumamoto University, 2-2-1 Honjo, Chuo-ku, Kumamoto, 860-0811, Japan

E-mail address: okadas@kumamoto-u.ac.jp (S. Okada)

Keywords

Primary effusion lymphoma (PEL) · Midkine inhibitor (iMDK) · Apoptosis · Cell cycle · AIDS

Abstract

Primary effusion lymphoma (PEL) is an aggressive B-cell non-Hodgkin lymphoma in immunocompromised individuals such as AIDS patients. PEL shows a poor prognosis (median survival time < 6 months) compared with other AIDS-related lymphomas, and is generally resistant to conventional treatments. Novel drugs for PEL treatment are required. Midkine inhibitor (iMDK) was previously found to suppress midkine protein expression. Interestingly, iMDK suppressed cell proliferation in PEL cell lines in a time- and dose-dependent manner, regardless of midkine gene expression. We examined the mechanism of iMDK on PEL. Importantly, iMDK strongly induced cell cycle arrest at the G2/M phase within 12 h of incubation and suppressed the p-CDK1 protein level, which is associated with the cell cycle checkpoint at G2/M, resulting in mitotic catastrophe with observation of multipolar division. After mitotic catastrophe, iMDK-treated PEL showed apoptosis with caspase-3, -8, and -9 activation at 24 h incubation. However, iMDK showed no effects on viral protein-activated signaling pathways such as JAK-STAT, PI3K-Akt and NF-κB, and HHV-8/KSHV gene expression in PEL. These results indicate that iMDK is a novel CDK1 inhibitor and a promising lead compound for PEL chemotherapy treatment.

1. Introduction

Primary effusion lymphoma (PEL) is an aggressive B-cell non-Hodgkin lymphoma that develops in immunocompromised individuals such as acquired immunodeficiency syndrome (AIDS)-patients and organ transplantation patients. It is a representative AIDS-associated disease, and accounts for approximately 4% of all human immunodeficiency virus (HIV)-associated non-Hodgkin lymphoma cases [1]. PEL develops in B-cells infected with human herpes virus-8 (HHV-8)/Kaposi's sarcoma-associated herpesvirus (KSHV). PEL develops in the body cavity fluid without detectable tumor masses and is characterized as a plasmablast, derived from post germinal center B-cells [2]. However, PEL cells usually lack expression of B-cell markers (CD19, CD20, CD79a, surface and cytoplasmic immunoglobulin) [1]. Viral proteins derived from the HHV-8/KSHV genome are essential for the survival and cell proliferation of PEL. For instance, v-FLIP, a viral homolog of FLICE inhibitory protein (c-FLIP), is essential for the survival of PEL by activating NF-κB through direct biding to IKKγ [3,4]. In addition, v-Cyclin, a viral homolog of cyclin D, forms active kinase complexes with CDK6 (cyclin-dependent kinase 6) to drive PEL cells to G1/S phase transition [5]. In addition, patients with PEL have very poor prognoses (median survival 6 months) under conventional treatment [6]. Since the HHV-8/KSHV genome locates in the host's nucleus, it is very hard to eradicate, and there is still no definitive medicine. A novel, effective drug is required for PEL treatment.

Midkine was first reported as a gene product during early differentiation stages of embryonal carcinoma cells and the mid-gestation period of mouse embryogenesis [7]. It is a 13 kDa protein and has rich basic amino acids. It forms a family with pleiotrophin, having about 50% amino acid sequence identity [8]. Midkine has various important

physiological roles in the growth, survival, inflammatory effect, and synthesis of cytokine after binding receptors such as ALK [9]. In the case of B cells, midkine maintains cell proliferation via the ALK pathway [10]. Importantly, midkine expression increases in several cancers such as lung, breast, prostate, and ovarian cancers [11]. Patients with high midkine expression have a worse prognosis than those with low midkine expression [12]. Therefore, midkine is associated with cancer development and is a promising marker of cancer progression in blood and urine [9].

Midkine inhibitor (iMDK) was first reported by screening for inhibition of the midkine protein level [13]. iMDK inhibited the growth of lung cancer *in vitro* by suppression of midkine, p-PI3K, and p-Akt protein levels. Furthermore, treatment with iMDK via i.p. injection inhibited the growth of human lung tumors in nude mice [13-15]. iMDK also inhibits tumor growth and angiogenesis in oral squamous cell carcinoma [16]. Midkine also expresses in lymphocytes and macrophages. Indeed, midkine expresses in several hematopoietic malignancies [17]. In addition, midkine regulates survival and homeostasis of normal peripheral mature B cells and chronic lymphocytic leukemia cells [18]. Therefore, targeting inhibition of midkine by iMDK might be a good strategy for cancer treatment. However, it remains to be clarified whether PEL express midkine.

In the present study, we elucidated the anti-cancer activity of iMDK on PEL *in vitro*.

2. Materials and methods

2.1. Reagents

Midkine inhibitor (iMDK) was purchased from Merck (Darmstadt, Germany). iMDK was dissolved in DMSO at 10 mM and stored at -30℃ until use. The chemical structure of iMDK is shown in Fig. 1A. Pan-caspase inhibitor, Q-VD-OPH was from R&D Systems,

Inc. (Minneapolis, MN).

2.2. Cell culture

BCBL-1 (AIDS Research and Reference Reagent Program, Division of AIDS, NIAID, NIH, Bethesda, MD), BC-1 (ATCC, Rockville, MD), GTO [19], TY-1 [20], and K562 (RIKEN Cell Bank, Tsukuba, Japan) cells were cultured at 37℃ in RPMI-1640 supplemented with 10% FBS, penicillin (100 IU/ml), and streptomycin (100 U/ml) in a humidified atmosphere containing 5% CO_2 and 95% air. 293 cells (American Type Culture Collection, Manassas, VA, USA) were cultured in DMEM supplemented with 10% FBS, penicillin (100 IU/ml), and streptomycin (100 U/ml).

2.3. Tetrazolium dye methylthiotetrazole (MTT) assay

BCBL-1, BC-1, GTO and TY-1 cells (2×10^4 cells/well in a 96-well plate) were incubated with various concentrations of iMDK at 37°C for 24–72 h. After incubation, MTT reagent was added, and cells were further incubated at 37°C for 3 h. The absorption value at 570 nm was measured using a microplate reader (iMark; Bio-Rad Laboratories Inc., Hercules, CA) after dissolving the formazan crystal.

2.4. Cell cycle analysis

BCBL-1 cells (4×10^5 cells/well in a 12-well plate) were incubated with various incubation times or concentrations of iMDK at 37°C. After incubation, treated-cells were washed with PBS^- and then stained with hypotonic buffer (0.1% sodium citrate, 0.2% NP-40, 50 μg/ml propidium iodide (PI), 0.25 mg/ml RNase) at 4°C for 30 min in the dark. The DNA content in each cell was analyzed by FACSCelesta (BD Bioscience, San Jose,

CA). Data were analyzed using FlowJo software version 10.4 (Tree Star, San Carlos, CA).

2.5. Annexin V biding assay

BCBL-1 cells (2×10^5 cells/well in a 24-well plate) were incubated with various concentrations of iMDK at 37°C for 24 h. After incubation, the treated cells were incubated with Pacific Blue™ Annexin V (BioLegend, 640918) and PI for 15 min at RT in the dark. The stained cells were analyzed by FACSCelesta. Data were analyzed as described above.

2.6. Western blotting

Total cell lysates were isolated from BCBL-1 cells treated with iMDK as described previously [21]. These lysates were subjected to sodium dodecyl sulfate-polyacrylamide gel electrophoresis. The proteins were then electrophoretically transferred to an Immobilon-P polyvinylidene difluoride membrane (Merck). Each protein was analyzed by western blotting using specific primary antibodies: anti-midkine mouse monoclonal antibody (a gift from Immuno Probe Co., Ltd., Saitama, Japan) and other antibodies listed in Supplementary Table 1. After incubation with horseradish peroxidase-labeled secondary antibodies, proteins were visualized using Chemi-Lumi One Super (Nacalai Tesque) and an ImageQuant LAS400 system (GE Healthcare, Chicago, IL).

2.7. Confocal microscopy analysis

BCBL-1 cells (2×10^5 cells/well in a 24-well plate) were incubated with 1000 nM of iMDK at 37°C for 24 h. After incubation, the treated cells (5×10^4 cells) were applied to CYTOSPIN 4 (Thermo) to make thin-layer cells on glass slides. The cells were fixed with

3.7% formalin for 20 min at RT, permeabilized with iced methanol for 10 min at -30°C, and blocked with 3% BSA for 1 h at RT. The cells were incubated with anti-α-tubulin antibody (α-Tubulin, sc-5286, Santa Cruz) for 1 h at 37°C, and then incubated with secondary antibody (A11034, Invitrogen) for 1 h at 37°C. After staining, the cells were incubated with DAPI (5 μg/ml) for 15 min at RT in the dark, and then mounted with SlowFade® Gold (Thermo). The samples were analyzed under a confocal laser-scanning microscope (FV-1000; Olympus Co., Tokyo, Japan).

2.8. Reverse transcription-polymerase chain reaction (RT-PCR)

To detect KSHV/HHV-8 gene expression, we performed RT-PCR using the method reported previously [21]. The PCR parameters for thermal cycling were as follows: 1 cycle of 70 sec at 95°C, 35 cycles of 55 sec at 93°C, 45 sec at 65°C, 40 sec at 72°C, 1 cycle of 100 sec at 72°C. The primers used in this study are listed in Supplementary Table 2. Each PCR reaction product (10 μl) was run on 1.5% agarose gels containing 0.5 μg/ml ethidium bromide, and observed by light capture (ATTO).

3. Results

3.1. iMDK suppresses cell proliferation of PEL, which does not express midkine

iMDK exerts its anti-cancer activities on lung and oral squamous cancer cells by targeting midkine protein expression [13, 16]. We examined the effect of iMDK on cell proliferation of PEL cell lines such as BCBL-1, BC-1, GTO, and TY-1, as estimated by MTT assay. Figure 1B shows that iMDK inhibited cell proliferation of PEL cell lines in a dose- and time-dependent manner. At 24 h incubation, the IC_{50} of iMDK was 472–932 nM (Fig. 1C). Furthermore, iMDK clearly showed lower IC_{50} at 48–72 h incubation

compared with 24 h. Especially, IC_{50} at 48 h incubation of BCBL-1, GTO and TY-1 cells were clearly decreased compared with 24 h. These data imply that iMDK induces cell death after 24 h of incubation. Since iMDK inhibited the cell proliferation of PEL, RT-PCR and western blotting were performed to detect midkine expression in PEL. We detected midkine expression of both mRNA and protein levels in the 293 cells used as a positive control (Fig. 1D and E). In addition, K562 cells, which were previously reported as positive for midkine expression [17], showed midkine expression, indicating that the expression might be stronger than that of 293 cells. In the case of PEL, contrary to our expectation, we failed to detect midkine expressions of either mRNA or protein. These data suggest that iMDK inhibited the cell proliferation of PEL regardless of the midkine expression. In subsequent experiments, we tried to elucidate this mechanism by using BCBL-1 cells.

3.2. iMDK strongly causes cell cycle arrest at the G2/M phase in PEL cell lines

Because the IC_{50} of iMDK on PEL drastically decreased during 24–48 h incubation, we hypothesized that iMDK may cause cell cycle arrest in PEL cell lines. Therefore, we analyzed the cell cycle of iMDK-treated PEL by FACS. iMDK strongly caused G2/M cell cycle arrest in a time- and dose-dependent manner in both BCBL-1 and GTO cells (Fig. 2A–D, Supplementary Fig. 1A–D). G2/M cell cycle arrest was observed after 6 h incubation in iMDK-treated BCBL-1 cells. Next, we examined CDK1 expression in PEL, which is involved in the cell cycle checkpoint at the G2/M phase. p-CDK1 makes a complex with Cyclin B1 to drive through the G2/M phase. iMDK decreased p-CDK1 but not CDK1 protein expression in a time-dependent manner (Fig. 2E). This result is consistent with data about the cell cycle (Fig. 2A, C). Confocal microscopy analysis was

performed to observe cell mitosis stained by α-tubulin, because CDK1 inhibition causes mitotic catastrophe [22]. iMDK-treated BCBL-1 showed aberrant mitotic features such as multipolar division. (Fig. 2F). These results suggest that iMDK caused cell cycle arrest at G2/M via inhibition of phosphorylation of CDK1, leading to mitotic catastrophe in BCBL-1 cells.

3.3. iMDK causes apoptosis of PEL

Apoptosis, necroptosis, and ferroptosis are well-known regulatory cell death pathways caused by drug treatments and infection [23]. To examine apoptosis of iMDK-treated PEL, we performed Annexin V-PI staining. iMDK increased apoptotic cells containing early (Annexin V single positive) and late (Annexin V and PI double positive) apoptotic cells in BCBL-1 and GTO cells in a dose-dependent manner at 24 h incubation. (Fig. 3A and B, Supplementary Fig. 2A and B). Next, we performed western blotting to detect cleaved caspase-3, -8, and -9, which are apoptosis-related proteins. iMDK showed their activation in BCBL-1 and GTO cells in a dose-dependent manner at 24 h incubation (Fig. 3C, Supplementary Fig. 2C). iMDK at 1000 nM induced all three caspase activations in BCBL-1 and GTO cells in a time-dependent manner (Fig. 3D, Supplementary Fig. 2D). To specifically examine whether iMDK induced apoptosis in PEL, we treated BCBL-1 cells with Q-VD-OPH, a pan-caspase inhibitor, before the addition of iMDK. The inhibitor decreased apoptotic cells in iMDK-treated PEL (Fig. 3E and F, Supplementary Fig. 2). Collectively, these results clearly show that iMDK induced apoptosis in PEL within 24 h incubation after cell cycle arrest.

3.4. iMDK shows no effects on viral protein-activated signaling pathway and HHV-

8/KSHV gene expressions in PEL

The HHV-8/KSHV genome locates in the nucleus of target cells after infection and forms latent or lytic phases. Latent genes such as LANA, v-FLIP and v-Cyclin maintain the viral genome and proliferation of infected cells. In the lytic phase, RTA and vIL-6 regulate lytic viral replication. Viral proteins derived from the HHV-8/KSHV genome constitutively activate signaling pathways such as JAK-STAT, PI3K-Akt, and NF-κB to promote cell proliferation, and are resistant to chemotherapy [1]. For example, vFLIP interacts with IKKγ and activates NF-κB translocation to the nucleus for cell proliferation [3, 4]. vIL-6 produced by PEL activates the JAK-STAT pathway of itself by autocrine signaling [24]. In previous studies, iMDK suppressed not only midkine but also the PI3K-Akt pathway in lung cancer cells [13, 14]. Accordingly, iMDK might suppress Akt phosphorylation in PEL. We examined the effects of iMDK on these signaling pathways in BCBL-1 cells such as Akt, STAT3 and NF-κB. The p-Akt473 protein level but not Akt was slightly decreased in iMDK-treated PEL at 24 h incubation (Fig. 4A). This probably resulted from death of BCBL-1 cells. However, p-STAT3, STAT, and p-NF-κB protein levels were not changed (Fig. 4B), suggesting that these were not the main targets of iMDK in PEL. Furthermore, iMDK showed no effects on HHV-8/KSHV gene expressions in BCBL-1 cells (Fig. 4C). This result suggests that iMDK inhibits cell proliferation of PEL without re-activation of HHV-8/KSHV gene expression; this is valuable for patients with PEL, who should not be put at risk of re-infection by exposure to HHV-8/KSHV particle re-activation resulting from iMDK treatment.

4. Discussion

In the present study, we mechanistically elucidated the mechanism whereby iMDK

inhibited cell proliferation via inducing G2/M cell cycle arrest and apoptosis. CDK1 and cyclin B play key roles in the G2/M checkpoint by forming a complex to drive the G2/M cell cycle phase. CDK1 has three phosphorylation sites, and only CDK1 phosphorylated at Thr161 is active. CDK1 at Thr161 is phosphorylated by CDK-activating kinase (CAK), which consists of CDK7 and Cyclin H [25]. Our results suggest that iMDK inhibits phosphorylation of CDK1 by inhibiting the enzymatic activity of CAK. However, it is still unclear whether iMDK inhibits enzymatic activity of CAK. We have to examine effects of iMDK on CDK7 and Cyclin H protein expression to elucidate their mechanism as next subject. Furthermore, we observed multi-centrosomes in iMDK-treated BCBL-1 cells, which were caused after G2/M cell cycle arrest by inhibition of phosphorylation of CDK1, resulting in mitotic catastrophe. Indeed, cleaved caspases in PEL were observed at 24 h after the start of treatment with iMDK. Therefore, apoptosis of iMDK-treated PEL was triggered by the mitotic catastrophe. There are several programmed cell death pathways: apoptosis, necroptosis, and ferroptosis [23]. According to Fig. 3, iMDK did not induce necroptosis of PEL because cells with necroptosis should show only PI positive in FACS analysis [26]. In addition, viral proteins such as vFLIP, vGPCR, K1 and vIL-6 activate signaling pathways to promote cytokine production and cell survival via NF-κB, PI3K-Akt and JAK-STAT pathways [1, 27]; these are therefore promising molecular targets for PEL treatment [1, 27]. Actually, inhibition of NF-κB induces apoptosis in PEL [28]. iMDK slightly suppressed phosphorylation of Akt but not phosphorylation of STAT3 or NF-κB. However, decreased protein levels resulted from the cell cycle arrest and activation of caspases. As such, phosphorylation of Akt is not a main target of iMDK.

iMDK has been shown to inhibit midkine protein expression but not its RNA. Although the mechanism is still unknown, iMDK may target the midkine protein directly

[13]. Indeed, previous studies reported that iMDK suppressed midkine protein expression in lung and oral squamous cancer cells [13, 16]. In our study, however, since PEL did not express midkine, this is a novel mechanism of iMDK. Therefore, iMDK can be classified as a novel cell cycle inhibitor. To further explore the potential of iMDK, as a next step we will perform an *in vivo* study. It is still unclear which proteins are bound by iMDK. Therefore, we will need to analyze iMDK-protein docking simulations. In addition, since iMDK has high hydrophobicity, its hydrophilicity must be increased by chemical modification for use *in vivo*.

PEL is an incurable AIDS-associated disease. Patients with PEL undergo CHOP (cyclophosphamide, hydroxydaunorubicin, oncovin and prednisone) chemotherapy, which is a conventional treatment applied to malignant lymphoma. However, since PEL is often resistant to CHOP chemotherapy, patients with PEL have a poor prognosis compared with other AIDS-related malignancies [6]. Recently, some promising candidate compounds have been reported for PEL treatment [27, 29]. These compounds target signaling pathway-associated proteins driven by KSHV-derived proteins. iMDK did not re-activate KSHV lytic genes in BCBL-1, suggesting that iMDK treatment does not expose patients to KSHV particles. This is an important benefit for patients with PEL who are at risk of re-infection during chemotherapy. We suggest that iMDK is a promising novel cell cycle inhibitor for PEL chemotherapy treatment. Our previous study developed highly immunodeficient, BALB/c Rag-$2^{-/-}$ $Jak^{-/-}$ (BRJ) mice [30], allowing us to create a PEL xenograft mouse model [29]. We hope to find an optimal combination with conventional therapy and perform an *in vivo* study as a next step.

In conclusion, iMDK acts as a cell cycle inhibitor against PEL and is a promising lead compound for PEL treatment.

CRediT author statement

Mikinori Ueno: Conceptualization, Methodology, Formal analysis, Investigation, Writing - Original Draft. Ryusho Kariya: Methodology, Investigation. Gunya Sittithumcharee: Investigation. Kodcharat Cheevapruk: Investigation. Seiji Okada: Resources, Writing - Review & Editing, Supervision, Funding acquisition. All data were generated in-house, and no paper mill was used. All authors agree to be accountable for all aspects of this work ensuring integrity and accuracy.

Conflict of interest

The authors have declared that there is no conflict of interest.

Acknowledgements

We are deeply grateful to Mr. Hiroshi Nomura (Immuno Probe Co., Ltd.) for anti-midkine mouse monoclonal antibody. We also thank Ms. Sawako Fujikawa for technical assistance and Ms. Michiko Teramoto for secretarial assistance.

Funding

This work was supported by International Collaborative Research Program: The e-ASIA Joint Research Program from the Japan Agency for Medical Research and Development (AMED). This work was also supported by a Grant-in-Aid for JSPS Research Fellows (18J00112).

References

[1] S. Okada, H. Goto, M. Yotsumoto, Current status of treatment for primary effusion lymphoma, Intractable Rare Dis. Res. 3 (2014) 65–74.

[2] R.G. Nador, E. Cesarman, A. Chadburn, D.B. Dawson, M.Q. Ansari, J. Sald, D.M. Knowles, Primary effusion lymphoma: a distinct clinicopathologic entity associated with the Kaposi's sarcoma-associated herpes virus, Blood. 88 (1996) 645–656.

[3] J. Molden, Y. Chang, Y. You, P.S. Moore, M.A. Goldsmith, A Kaposi's sarcoma-associated herpesvirus-encoded cytokine homolog (vIL-6) activates signaling through the shared gp130 receptor subunit, J. Biol. Chem. 272 (1997) 19625–19631.

[4] S. Uddin, A.R. Hussain, K.A. AI-Hussein, P.S. Manogaran, A. Wickrema, M.I. Gutierrez, K.G. Bhatia, Inhibition of phosphatidylinositol 3'-kinase/Akt signaling promotes apoptosis of primary effusion lymphoma cells, Clin. Cancer Res. 11 (2005) 3102–3108.

[5] C. Swanton, D.J. Mann B. Fleckenstein, F. Neipel, G. Peters, N. Jones, Herpes viral cyclin/Cdk6 complexes evade inhibition by CDK inhibitor proteins, Nature. 390 (1997) 184–187.

[6] S. Hagiwara, H. Nagai, J. Tanaka, S. Okada, The current state of human immunodeficiency virus-associated lymphoma in Japan: a nationwide retrospective study of the Japanese Society of Hematology Blood Disease Registry, Int. J. Hematol. 110 (2019) 244–249.

[7] K. Kadomatsu, M. Tomomura, T. Muramatsu, cDNA cloning and sequencing of a new gene intensely expressed in early differentiation stages of embryonal carcinoma cells and in mid-gestation period of mouse embryogenesis. Biochem. Biophys. Res. Commun. 151 (1988) 1312–1318.

[8] T. Muramatsu, Midkine and pleiotrophin: Two related proteins involved in

development, survival, inflammation and tumorigenesis. J. Biochem. 132 (2002) 359–371.

[9] P.S. Filippou, G.S. Karagiannis, A. Constantinidou, Midkine (MDK) growth factor: a key player in cancer progression and a promising therapeutic target, Oncogene. 39 (2020) 2040–2054.

[10] E. Koren, Y. Fuchs, Modes of regulated cell death in cancer, Cancer Discov. 11 (2021) 245–265.

[11] T. Muramatsu, Midkine, a heparin-binding cytokine with multiple roles in development, repair and diseases. Proc. Jpn. Acad. Ser. B. 86 (2010) 410-425.

[12] H. Shimada, Y. Nabeya, M. Tagawa, S. Okazumi, H. Matsubara, K. Kadomatsu, T. Muramatsu, S. Ikematsu, S. Sakuma, T. Ochiai, Preoperative serum midkine concentration is a prognostic marker for esophageal squamous cell carcinoma. Cancer Sci. 94 (2003) 628–632.

[13] H. Hao, Y. Maeda, T. Fukazawa, T. Yamatsuji, M. Takaoka, X.H. Bao, J. Matsuoka, T. Okui, T. Shimo, N. Takigawa, Y. Tomono, M. Nakajima, I.M. Fink-Baldauf, S. Nelson, W. Seibel, R. Papoian, J.A. Whitsett, Y. Naomoto, Inhibition of the growth factor MDK/Midkine by a novel small molecule compound to treat non-small cell lung cancer, PLoS One. 8 (2013) e71093.

[14] N. Ishida, T. Fukazawa, Y. Maeda, T. Yamatsuji, K. Kato, K. Matsumoto, T. Shimo, N. Takigawa, J.A. Whitsett, Y. Naomoto, A novel PI3K inhibitor iMDK suppresses non-small cell lung cancer cooperatively with a MEK inhibitor. Exp. Cell Res. 335 (2015) 197–206.

[15] D.H. Shin, J.Y. o, S.H. Kim, M. Choi, C. Han, B.K. Choi, S.S. Kim, Midkine is a potential therapeutic target of tumorigenesis, angiogenesis, and metastasis in non-

small cell lung cancer, Cancers. 12 (2020) 2402.

[16] M. Masui, T. Okui, T. Shimo, K. Kabatake, T. Fukazawa, K. Matsumoto, N. Kurio, S. Ibaragi, Y. Naomoto, H. Nagatsuka, A. Sasaki, Novel midkine inhibitor iMDK inhibits tumor growth and angiogenesis in oral squamous cell carcinoma, Anticancer Res. 36 (2016) 2775–2782.

[17] H. Kato, K. Watanabe, M. Murari, C. Isogai, T. Kinoshita, H. Nagai, H. Ohashi, T. Nagasaka, K. Kadomatsu, H. Muramatsu, T. Muramatsu, H. Saito, Naoyoshi, Mori, T. Murase, Midkine expression in Reed-Sternberg cells of Hodgkin's disease. Leuk. Lymphoma. 37 (2000) 415–424.

[18] S. Cohen, I. Shachar, Midkine as a regular of B cell survival in health and diseases. Br. J. Pharmacol. 171 (2014) 888–895.

[19] H. Goto, Y. Kojima, H. Nagai, S Okada, Establishment of a CD4-positive cell line from an AIDS-related primary effusion lymphoma, Int. J. Hematol. 97 (2013) 624–633.

[20] H. Katano, Y. Hoshino, Y. Morishita, T. Natamura, H. Satoh, A. Iwamoto, B. Herndier, S. Mori, Establishing and characterizing a CD30-positive cell line harboring HHV-8 from a primary effusion lymphoma, J. Med. Virol. 58 (1999) 394–401.

[21] R. Kariya, M. Taura, S. Suzu, H. Kai, H. Katano, S. Okada, HIV protease inhibitor Lopinavir induces apoptosis of primary effusion lymphoma cells via suppression of NF-κB pathway, Cancer Lett. 342 (2014) 52-59.

[22] M. Kawakami, L.M. Mustachio, E. Dmitrovsky, Engaging anaphase catastrophe mechanisms to eradicate aneuploid cancers. Mol. Cancer Ther. 17 (2018) 724–731.

[23] E. Koren, Y. Fuchs, Modes of regulated cell death in cancer. Cancer Discov. 11 (2021) 245–265.

[24] K.D. Jones, Y. Aoki, Y. Chang, P.S. Moore, R. Yarchoan, G. Tosato, Involvement of interleukin-10 (IL-10) and viral IL-6 in the spontaneous growth f Kaposi's sarcoma herpesvirus-associated infected primary effusion lymphoma cells. Blood. 94 (1999) 2871–2879.

[25] D. Desai, H.C. Wessling, R.P. Fisher, D.O. Morgan, Effects of phosphorylation by CAK on cyclin binding by CDC2 and CDK2. Mol. Cell. Biol., 15 (1995) 345–350.

[26] Y. Li, X, Tian, X. Liu, P. Gong, Bufalin inhibits human breast cancer tumorigenesis by inducing cell death through the ROS-mediated RIP1/RIP3/PARP-1 pathways. Carcinogenesis. 39 (2018) 700–707.

[27] K. Shimada, F. Hayakawa, H. Kiyoi, Biology and management of primary effusion lymphoma, Blood. 132 (2018) 1879–1888.

[28] S.A. Keller, E.J. Schattner, E. Cesarman, Inhibition of NF-κB induces apoptosis of KSHV-infected primary effusion lymphoma cells. Blood, 96 (2000) 2537–2542.

[29] M. Ueno, R. Kariya, G. Sittithumcharee, S. Okada, Cucurbitacin B induces apoptosis of primary effusion lymphoma via disruption of cytoskeletal organization, Phytomedicine. 85 (2021) 153545.

[30] A. Ono, S. Hattori, R. Kariya, S. Iwanaga, M. Taura, H. Harada, S. Suzu, S. Okada, Comparative study of human hematopoietic cell engraftment in Balb/c and C57BL/6 strain Rag-2/Jak3 double deficient mice. J. Biome. Biotechnol. 2011 (2011) 539748.

Figure legends

Fig. 1 iMDK inhibits cell proliferation of PEL. (**A**) Chemical structure of iMDK. (**B**) PEL cell lines were cultured with various concentrations of iMDK or for various times. Cell proliferation was estimated by MTT assay. (**C**) shows IC_{50} of iMDK. (**D**) Total RNA was extracted from 293, K562, and PEL cell lines, reverse-transcribed to cDNA, and amplified by PCR in order to detect mRNA of midkine. (**E**) Whole protein was extracted from 293, K562, and PEL cell lines. Midkine protein was detected by western blotting.

Fig. 2 iMDK causes cell cycle arrest at G2/M in PEL. (**A**) BCBL-1 cells were incubated with 1000 nM of iMDK for 0–12 h. The DNA contents were analyzed by flow cytometry. (**B**) BCBL-1 cells were cultured with various concentrations of iMDK for 12 h. The DNA contents were analyzed by flow cytometry. (**C**) and (**D**) summarize the data of (A) and (B), respectively. (**E**) BCBL-1 cells were incubated with 1000 nM of iMDK for 0–12 h. p-CDK1 Thr 161 and CDK1 were detected by western blotting. (**F**) BCBL-1 cells were incubated with 1000 nM of iMDK for 24 h. α-tubulin was observed by laser confocal microscopy.

Fig. 3 iMDK induces apoptosis in PEL. (**A, B**) BCBL-1 cells were cultured with various concentrations of iMDK for 24 h. Annexin V-PI staining was performed and analyzed by flow cytometry. (**C**) BCBL-1 cells were cultured with various concentrations of iMDK for 24 h. Each protein was detected by western blotting. (**D**) BCBL-1 cells were treated with 1000 nM of iMDK for 0–24 h. Each protein was detected by western blotting. (**E, F**) BCBL-1 cells were treated with 20 μM of caspase inhibitor, Q-VD-OPH, for 2 h before addition of 1000 nM of iMDK. After 24 h incubation, Annexin V-PI staining was

performed and analyzed by flow cytometry.

Fig. 4 iMDK shows no effects on signaling pathway and HHV-8/KSHV gene expression in PEL. (**A, B**) BCBL-1 cells were cultured with 1000 nM of iMDK for 0–24 h. Each protein was detected by western blotting. (**C**) BCBL-1 cells were cultured with 1000 nM of iMDK for 0–12 h. Each KSHV/HHV-8 gene was analyzed by RT-PCR.

Fig. 1

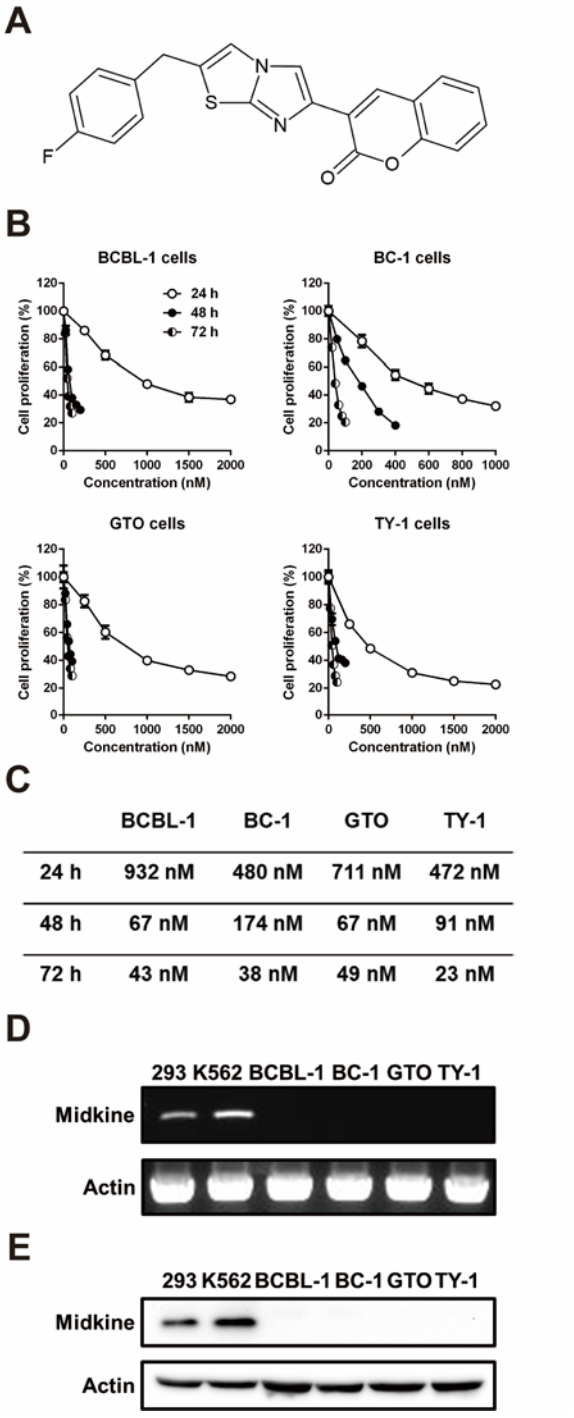
A
F
S
N
N
O
O
B
BCBL-1 cells
BC-1 cells
GTO cells
TY-1 cells
24 h
48 h
72 h
Cell proliferation (%)
Concentration (nM)
C
BCBL-1 BC-1 GTO TY-1
24 h 932 nM 480 nM 711 nM 472 nM
48 h 67 nM 174 nM 67 nM 91 nM
72 h 43 nM 38 nM 49 nM 23 nM
D
293 K562 BCBL-1 BC-1 GTO TY-1
Midkine
Actin
E
293 K562 BCBL-1 BC-1 GTO TY-1
Midkine
Actin

Fig. 2

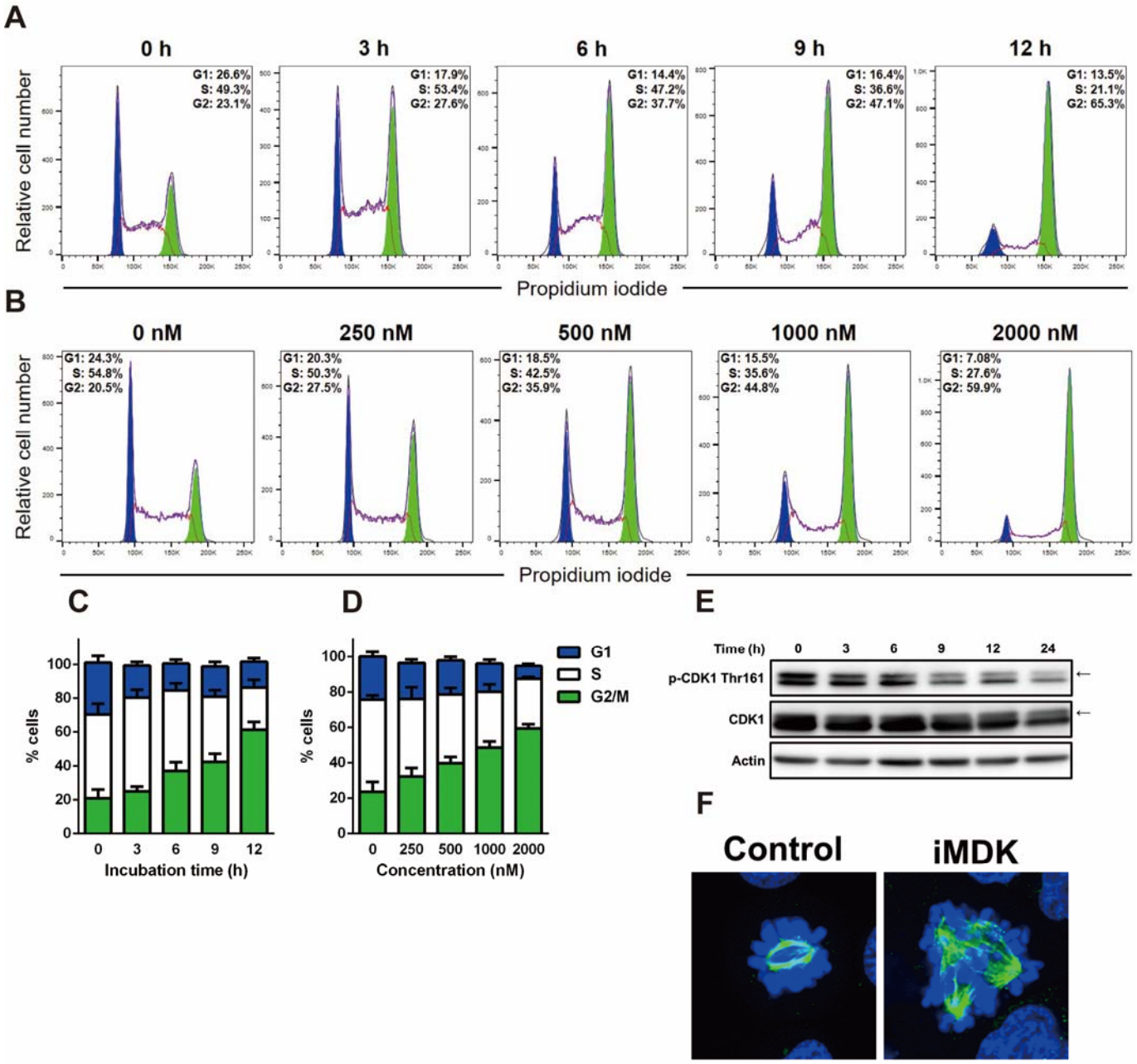
A
0 h
3 h
6 h
9 h
12 h
G1: 26.6%
S: 49.3%
G2: 23.1%
G1: 17.9%
S: 53.4%
G2: 27.6%
G1: 14.4%
S: 47.2%
G2: 37.7%
G1: 16.4%
S: 36.6%
G2: 47.1%
G1: 13.5%
S: 21.1%
G2: 65.3%
Relative cell number
Propidium iodide
B
0 nM
250 nM
500 nM
1000 nM
2000 nM
G1: 24.3%
S: 54.8%
G2: 20.5%
G1: 20.3%
S: 50.3%
G2: 27.5%
G1: 18.5%
S: 42.5%
G2: 35.9%
G1: 15.5%
S: 35.6%
G2: 44.8%
G1: 7.08%
S: 27.6%
G2: 59.9%
Relative cell number
Propidium iodide
C
% cells
Incubation time (h)
D
% cells
Concentration (nM)
G1
S
G2/M
E
Time (h)
p-CDK1 Thr161
CDK1
Actin
F
Control
iMDK

Fig. 3

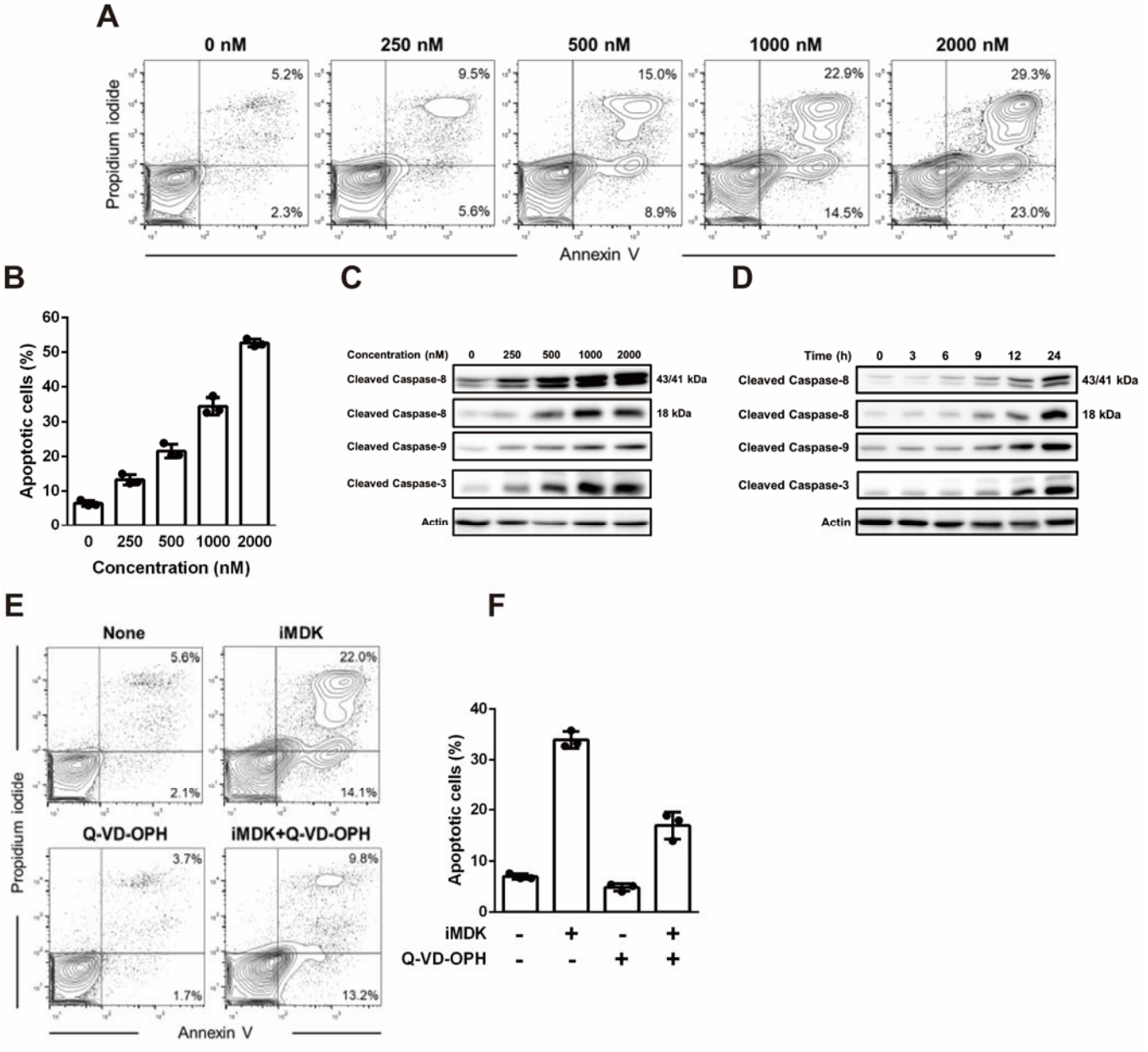
A
0 nM
250 nM
500 nM
1000 nM
2000 nM
Propidium iodide
5.2%
2.3%
9.5%
5.6%
15.0%
8.9%
22.9%
14.5%
29.3%
23.0%
Annexin V
B
Apoptotic cells (%)
0
10
20
30
40
50
60
0
250
500
1000
2000
Concentration (nM)
C
Concentration (nM) 0 250 500 1000 2000
Cleaved Caspase-8
43/41 kDa
Cleaved Caspase-8
18 kDa
Cleaved Caspase-9
Cleaved Caspase-3
Actin
D
Time (h) 0 3 6 9 12 24
Cleaved Caspase-8
43/41 kDa
Cleaved Caspase-8
18 kDa
Cleaved Caspase-9
Cleaved Caspase-3
Actin
E
None
iMDK
5.6%
2.1%
22.0%
14.1%
Q-VD-OPH
iMDK+Q-VD-OPH
3.7%
1.7%
9.8%
13.2%
Propidium iodide
Annexin V
F
Apoptotic cells (%)
0
10
20
30
40
iMDK - + - +
Q-VD-OPH - - + +

Fig. 4

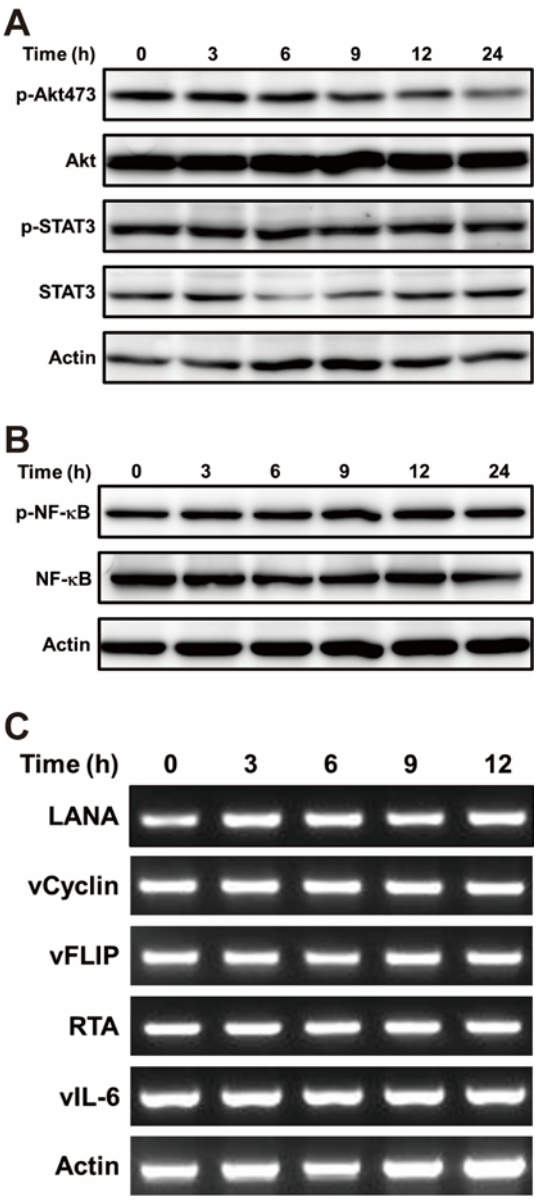
A
Time (h) 0 3 6 9 12 24
p-Akt473
Akt
p-STAT3
STAT3
Actin
B
Time (h) 0 3 6 9 12 24
p-NF-κB
NF-κB
Actin
C
Time (h) 0 3 6 9 12
LANA
vCyclin
vFLIP
RTA
vIL-6
Actin

Highlights

- iMDK inhibited cell proliferation of PEL cells
- PEL cells do not express midkine
- iMDK induced cell cycle arrest at G2/M arrest in PEL cells
- iMDK caused apoptosis of PEL cells via caspase activation

Acknowledgements

We are deeply grateful to Mr. Hiroshi Nomura (Immuno Probe Co., Ltd.) for anti-midkine mouse monoclonal antibody. We also thank Ms. Sawako Fujikawa for technical assistance and Ms. Michiko Teramoto for secretarial assistance.

Conflict of interest

The authors have declared that there is no conflict of interest.

Mikinori Ueno[a,d], Ryusho Kariya[a], Sittithumcharee Gunya[a,b], Kodcharat Cheevapruk[a,b,c], Seiji Okada[a,b,*]

Division of Hematopoiesis, [a]Joint Research Center for Human Retrovirus Infection, [b]Graduate School of Medical Sciences, Kumamoto University, 2-2-1 Honjo, Chuo-ku, Kumamoto, 860-0811, Japan

[c]Department of Pharmacology, Faculty of Medicine Siriraj Hospital, Mahidol University, Bangkok 10700, Thailand

[d]Current address: Graduate School of Fisheries and Environmental Studies, Nagasaki University, 1-14 Bunkyo-machi, Nagasaki, 852-8521, Japan

Supplementary Table 1. List of antibodies used in this study

Antibody	Company	Code	Dilution
Cleaved Caspase-3 (Asp175) antibody	Cell Signaling Technology	9661	1:1000
Cleaved Caspase-8 (Asp391) (18C8) rabbit mAb	Cell Signaling Technology	9496	1:1000
Cleaved Caspase-9 (Asp315) (D819E) rabbit mAb	Cell Signaling Technology	20750	1:1000
Phospho-cdc2 (Thr161) antibody	Cell Signaling Technology	9114	1:1000
Akt (pan) (C67E7) rabbit mAb	Cell Signaling Technology	4691	1:1000
Phospho-Akt (Ser473) (D9E) XP® rabbit mAb	Cell Signaling Technology	4060	1:1000
Phospho-NF-κB p65 (Ser536) (93H1) rabbit mAb	Cell Signaling Technology	3033	1:1000
Anti-mouse IgG, HRP-linked antibody	Cell Signaling Technology	7076	1:2000
Anti-rabbit IgG, HRP-linked antibody	Cell Signaling Technology	7074	1:2000
Actin antibody (C-2)	Santa Cruz	sc-8432	1:1000
Stat3 antibody (F-2)	Santa Cruz	sc-8019	1:1000
NFκB p65 antibody (C-20)	Santa Cruz	sc-372	1:1000
Cdc2 p34	Santa Cruz	sc-54	1:1000
Purified anti-STAT3 pshospho (Tyr705) antibody	BioLegend	651001	1:1000

Supplementary Table 2. Primers for RT-PCR

Primers	Direction	
LANA1	Forward	5'-GAAGTGGATTACCCTGTTGTTAGC-3'
LANA1	Reverse	5'-TTGGATCTCGTCTTCCATCC-3'
v-Cyclin	Forward	5'-GATAATAGAGGCGGGCAATG-3'
v-Cyclin	Reverse	5'-TAAAGCAGGTGTCCAAAGAA-3'
v-FLIP	Forward	5'-ATTGACATTAGGGCATCC-3'
v-FLIP	Reverse	5'-AAAGGAGGAGGGCAGGTT-3'
RTA	Forward	5'-GCCCTCTGCCTTTTGGTT-3'
RTA	Reverse	5'-GATGATGCTGACGGTGTG-3'
vIL-6	Forward	5'-AAAACACGCACCGCTTGACCTG-3'
vIL-6	Reverse	5'-TTCACTGCTGGTATCTGGAACG-3'
Actin	Forward	5'-GTGGGGCGCCCCAGGCACCA-3'
Actin	Reverse	5'-CTCCTTAATGTCACGCACGATTTC-3'

Supplementary Figure 1

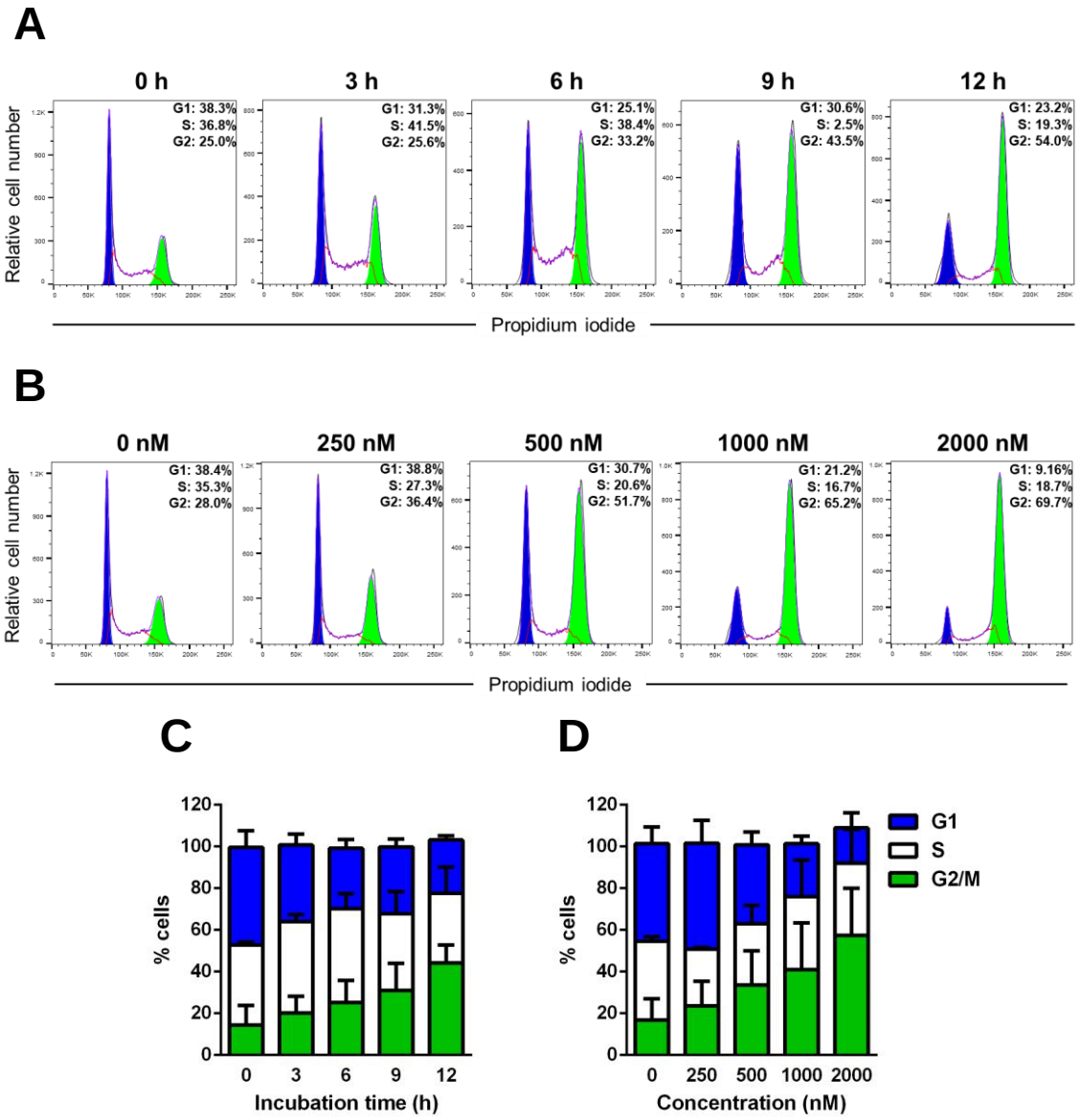

GTO cells (4×10^5 cells/well in a 12-well plate) were incubated with a varying incubation time or concentration of iMDK at 37° C. After incubation, treated-cells were washed by PBS^- and then stained with hypotonic buffer (0.1% sodium citrate, 0.2% NP-40, 50 μg/ml propidium iodide (PI), 0.25 mg/ml RNase) at 4° C for 30 min in the dark. The DNA content in each cell was analyzed on FACSCelesta (BD Bioscience, San Jose, CA). Data were analyzed on FlowJo software version 10.4 (Tree Star, San Carlos, CA). (**A**) GTO cells were incubated with 1000 nM of iMDK for 0–12 h. The DNA contents were analyzed on flow cytometry. (**B**) GTO cells were cultured with a varying concentration of iMDK for 12 h. The DNA contents were analyzed on flow cytometry. (**C**) and (**D**) summarize the data of (A) and (B), respectively.

Supplementary Figure 2

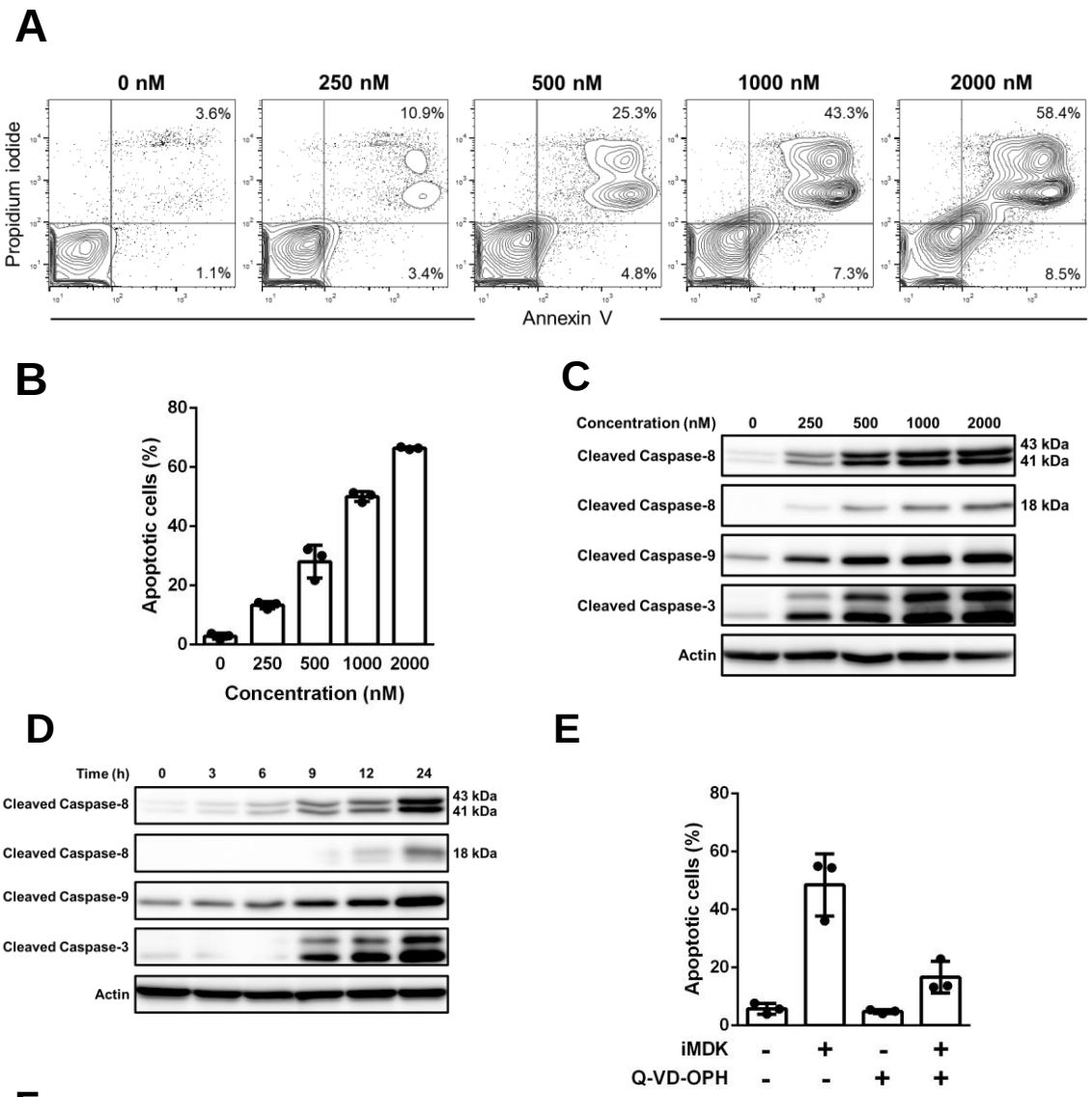

GTO cells (2 × 10^5 cells/well in a 24-well plate) were incubated with varying concentration of iMDK at 37° C for 24 h. After incubation, the treated cells were incubated with Pacific blue™ Annexin V (BioLegend, 640918) and PI for 15 min at RT in the dark. The stained cells were analyzed on FACSCelesta. (**A, B**) GTO cells were cultured with a varying concentration of iMDK for 24 h. Annexin V-PI staining was performed and analyzed on flow cytometry. (**C**) GTO cells were cultured with a varying concentration of iMDK for 24 h. Each protein was detected by western blotting. (**D**) GTO cells were treated with 1000 nM of iMDK for 0–24 h. Each protein was detected by western blotting. (**E, F**) GTO cell were treated with 20 μM of caspase inhibitor, Q-VD-OPH, for 2 h before addition of 1000 nM of iMDK. After 24 h incubation, Annexin V-PI staining was performed and analyzed on flow cytometry.